PHYSICAL REVIEW B VOLUME 29, NUMBER 1 1 JANUARY 1984

Quasiparticle density of states in superconducting alloys with localized states within the gap

E. Schachinger
Institut für Theoretische Physik der Technischen Universität Graz, A-8010 Graz, Austria

J. P. Carbotte
Physics Department, McMaster University, Hamilton, Ontario L8S 4M1, Canada
(Received 15 July 1983)

We present results of real-frequency-axis strong-coupling calculations for the quasiparticle density of states of superconducting alloys with localized states within the energy gap. These states arise from spin-flip scattering by paramagnetic impurities treated within the T-matrix approach of Rusinov and Shiba. Comparison of our results with previous imaginary-frequency-axis Eliashberg calculation and with the results of BCS-theory calculations reveals differences in the predicted structures within and near the main gap edge. It is also found that the quasiparticle density of states in the phonon energy range is strongly affected by the impurities.

I. INTRODUCTION

When the spin-flip scattering of a superconducting electron off a paramagnetic impurity is strong, it is necessary to go to a scattering-matrix formulation as was done by Shiba[1,2] and Rusinov[3,4] (SR) instead of the second-order perturbation treatment of Abrikosov and Gor'kov[5] (AG). The most striking feature of this generalization of AG theory is the existence of bands of states within the original energy gap. Many works, both experimental and theoretical, now exist,[6–13] including evidence for multiple spherical-harmonic-level scattering. These works are all based on the BCS-theory description of the superconducting state.

The first generalization of magnetic alloy theory to include strong-coupling effects within Eliashberg theory[14] was given by Schachinger.[15] His work deals with the imaginary-frequency-axis formulation of the Eliashberg equations as does also the work of Schachinger, Daams, and Carbotte[16] based on AG theory. In this formulation the quasiparticle density of states is obtained indirectly from an analytic continuation to the real-frequency axis, of the imaginary-axis numerical results, making use of a Padé-approximant scheme as pioneered by Vidberg and Serene.[17] For several pure metals these authors show that a great deal of agreement can be achieved between their analytical continuations for the gaps and existing real-axis gaps but that not all details, particularly at higher energies, can be reproduced in this way. Nevertheless, for alloys with SR magnetic impurities the analytic continuation solution work of Schachinger[15] reveals structures within the gap similar to those predicted in BCS theories, although differences are found. For Pb-Mn alloys the Eliashberg results give better agreement with tunneling experiments, although it should be kept in mind that some smearing of the predicted structure within the gap must come from the limitations of the Padé-approximant technique itself.

In this paper we present the first strong-coupling results for Pb and In using the SR model for magnetic impurities incorporated into the real axis formulation of the Eliashberg equations. Our aim is to establish differences with BCS-theory models and also check on the effectiveness of analytic continuation techniques.

In Sec. II we write down the real-axis Eliashberg equations generalized to include paramagnetic impurities within the SR model extended to include multiple levels. These form the basis of this paper. Numerical solutions are presented for the real and imaginary parts of the gap and of the renormalization functions for a series of Pb-Mn alloys and comparison is made with pure Pb. In Sec. III we present the quasiparticle density of states for several sets of scattering parameters equal to some for which BCS-theory results already exist in the literature so that comparison can be made. A detailed comparison with the previous strong-coupling work of Schachinger is also presented. A new result which is absent in BCS-theory formulations is given in Sec. IV where the phonon region of the quasiparticle density of states is considered in detail. Conclusions can be found in Sec. V.

II. REAL-AXIS EQUATIONS

As the imaginary-axis version of the Eliashberg equations with paramagnetic impurities included in the SR model has been derived by Schachinger and since the technique for going to the real axis is the same as when no impurities are present, we simply write down the real-axis version. They are two coupled nonlinear integral equations for a frequency-dependent complex gap $\Delta(\omega)$ and renormalization function $Z(\omega)$. At temperature T, they are

$$\Delta(\omega,T)Z_s(\omega,T)=\int_0^{\omega_c}d\omega'\mathrm{Re}\left[\frac{\Delta(\omega',T)}{[\omega'^2-\Delta^2(\omega',T)]^{1/2}}\right]\times\int_0^{\infty}d\nu\,\alpha^2(\nu)F(\nu)\left[[n(\nu)+f(-\omega')]\left[\frac{1}{\omega+\omega'+\nu+i0^+}-\frac{1}{\omega-\omega'-\nu+i0^+}\right]-[n(\nu)+f(\omega')]\left[\frac{1}{\omega+\nu-\omega'+i0^+}-\frac{1}{\omega-\nu+\omega'+i0^+}\right]\right]-\mu^*\int_0^{\omega_c}d\omega'\mathrm{Re}\left[\frac{\Delta(\omega',T)}{[\omega'^2-\Delta^2(\omega',T)]^{1/2}}\right][1-f(\omega')]-i\frac{\Delta(\omega,T)}{[\omega^2-\Delta^2(\omega,T)]^{1/2}}\sum_{l=0}^{\infty}(2l+1)\alpha_l\frac{\epsilon_l}{1+\epsilon_l}\frac{\omega^2-\Delta^2\omega,T)}{\omega^2-\epsilon_l^2\Delta^2(\omega,T)}\tag{1}$$

and

$$[1-Z_s(\omega,T)]\omega=\int_0^{\infty}d\omega'\mathrm{Re}\left[\frac{\omega'}{[\omega'^2-\Delta^2(\omega',T)]^{1/2}}\right]\times\int_0^{\infty}d\nu\,\alpha^2(\nu)F(\nu)\left[[n(\nu)+f(-\omega')]\left[\frac{1}{\omega+\omega'+\nu+i0^+}+\frac{1}{\omega-\omega'-\nu+i0^+}\right]+[n(\nu)+f(\omega')]\left[\frac{1}{\omega-\omega'+\nu+i0^+}+\frac{1}{\omega-\nu+\omega'+i0^+}\right]\right]-i\frac{\omega}{[\omega^2-\Delta^2(\omega,T)]^{1/2}}\sum_{l=1}^{\infty}(2l+1)\alpha_l\frac{1}{1+\epsilon_l}\frac{\omega^2-\Delta^2(\omega,T)}{\omega^2-\epsilon_l^2\Delta^2(\omega,T)}\,.\tag{2}$$

In these two equations $i0^+$ is a small positive imaginary part, $n(\nu)$ is the Bose-Einstein thermal factor, $f(\omega)$ is the Fermi-Dirac distribution, and $\alpha^2(\omega)F(\omega)$ is the electron-phonon spectral density characteristic of the pure metal.[18] It is assumed not to be directly modified by the introduction of the paramagnetic impurities. The term μ^*, also assumed not to be significantly different in the alloy, describes the Coulomb repulsions with a cutoff at ω_c. The impurity parameters ϵ_l are related to the spin up (S_l^+) and spin down (S_l^-) phase shift in the lth partial-wave channel given by $\epsilon_l=\cos(S_l^+-S_l^-)$ and α_l is given by

$$\alpha_l=\frac{n_I}{2\pi N(0)}(1-\epsilon_l^2)\,,\tag{3}$$

where n_I is the paramagnetic impurity concentration and $N(0)$ the density of electron states at the Fermi surface for one spin. Kunz and Ginsberg[10] have given band-structure calculations of these parameters for several impurities and hosts. The α_l's are related to the single pair-breaking parameter (α) entering the AG theory by

$$\alpha=\sum_{l=0}^{\infty}(2l+1)\alpha_l\,.\tag{4}$$

In fact, the equation for T_c is the same in SR theory as in AG theory.

To emphasize the fact that strong-coupling theory can give very different results from BCS theory for certain quantities, we recall that at the critical concentration Schachinger, Daams, and Carbotte[16] found for Pb, that in strong coupling the pair-breaking parameter

$$\alpha_c=2.8T_{c0}\,,$$

where T_{c0} is the pure-metal critical temperature, as opposed to $0.89T_{c0}$ in BCS theory and 2.27 in the "square-well model." In this last case, the BCS-theory formula for α_c is simply renormalized by an additional factor of $1+\lambda=2.55$.

From formulas (3) and (4) it follows that the impurity concentration is related to α by

$$n_I=\frac{2\pi N(0)\alpha}{\sum_{l'}(2l'+1)(1-\epsilon_{l'}^2)}\,.\tag{5}$$

In Fig. 1 we show n_I for Pb with two different models (to be studied later) of the paramagnetic impurity as a function of T_c/T_{c0}. In the first model $\epsilon_0=0.25$ and $\epsilon_1=0.8$, and in the second model, $\epsilon_0=0.985$, $\epsilon_1=0.967$, and $\epsilon_2=0.970$. We see that the three curves—namely BCS theory, the square-well model, and the full Eliashberg theory—differ radically from each other, illustrating well the need for the present study. It is not at all clear that a BCS-theory model can be employed unaltered in studies of the quasiparticle density of states in superconducting alloys with random paramagnetic impurities.

We have solved Eqs. (1) and (2) using the $\alpha^2(\omega)F(\omega)$ obtained by Rowell and McMillan[18] for the case of pure Pb and several models for the paramagnetic impurities. In Figs. 2(a) and 2(b) we show a series of curves for the

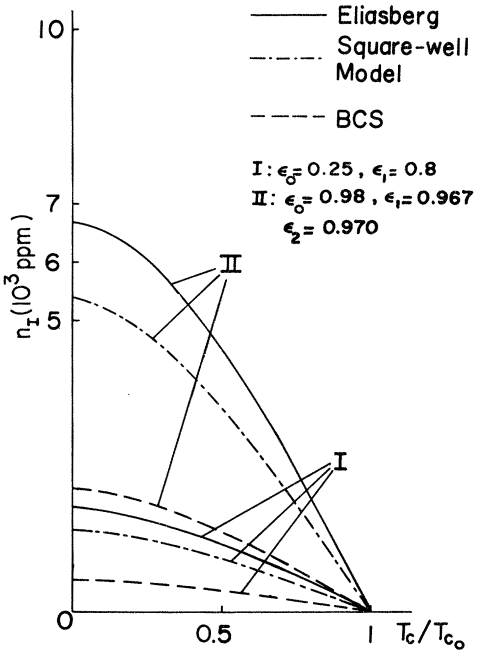

FIG. 1. Impurity concentration n_I in ppm as a function of the alloy to the pure-metal critical temperature T_c/T_c^0 for two models of paramagnetic impurities in Pb. Model I has $\epsilon_2=0.25$ and $\epsilon_1=0.8$, and model II has $\epsilon_0=0.985$, $\epsilon_1=0.967$, and $\epsilon_2=0.970$. Three different models for the superconducting state are considered. Dashed line is for BCS theory, dashed-dotted line is the square-well model, and solid curve is the Eliashberg result.

real and imaginary part of the gap $\Delta(\omega)$ and the renormalization function $Z(\omega)$ at zero temperature for a model in which $\epsilon_0=0.25$ and $\epsilon_1=0.8$. The various runs are labeled according to the ratio T_c/T_{c0}, the alloy to pure-Pb critical temperature. Considering the gap first, we note that for pure Pb the imaginary part of $\Delta(\omega)$ is zero below the gap edge defined by

$$\mathrm{Re}\Delta(\omega=\Delta_0)=\Delta_0 .$$

This is no longer the case when paramagnetic impurities are present. It is seen that at small ω the imaginary part of $\Delta(\omega)$ is finite and negative while at higher energies it follows more closely the pure-Pb case although its size is progressively reduced.

The real part of the gap is also affected. It is changed in two major respects. First, at energies well below the pure-Pb gap edge, Δ_0, structure is observed and the gap is greatly changed. At higher energy the modifications are not so pronounced but there is a general decerease in the phonon structure which we will later see is reflected in the quasiparticle density of states.

For clarity we have included in Fig. 2(b), which refers to the renormalization function $Z(\omega)$, only two cases, namely pure Pb and the alloy with $T_c/T_{c0}=0.42$. Some change in the real and imaginary parts of $Z(\omega)$ is seen in the phonon-energy region, but the most important difference between alloy and pure metal is the low-ω behavior of the imaginary part of Z, which has acquired a $1/\omega$-type dependence. This is not unexpected as can be easily seen from Eq. (2) taken, for simplicity, in the normal state. In that case the impurity part of the right-hand side of the equation reduces to ($\omega>0$)

$$-i\sum_{l=0}^{\infty}(2l+1)\alpha_l\frac{1}{1+\epsilon_l} , \tag{6}$$

which is pure imaginary leading to a term of the form

$$-\frac{i}{\omega}\sum_{l=0}^{\infty}\frac{2l+1}{2\pi N(0)}n_I(1-\epsilon_l) \tag{7}$$

in the imaginary part of $Z(\omega)$ since it is $[1-Z(\omega)]\omega$ that appears on the left-hand side.

III. QUASIPARTICLE DENSITY OF STATES

The quasiparticle density of states $N(\omega)$ which can be measured in tunneling experiments is related only to $\Delta(\omega)$

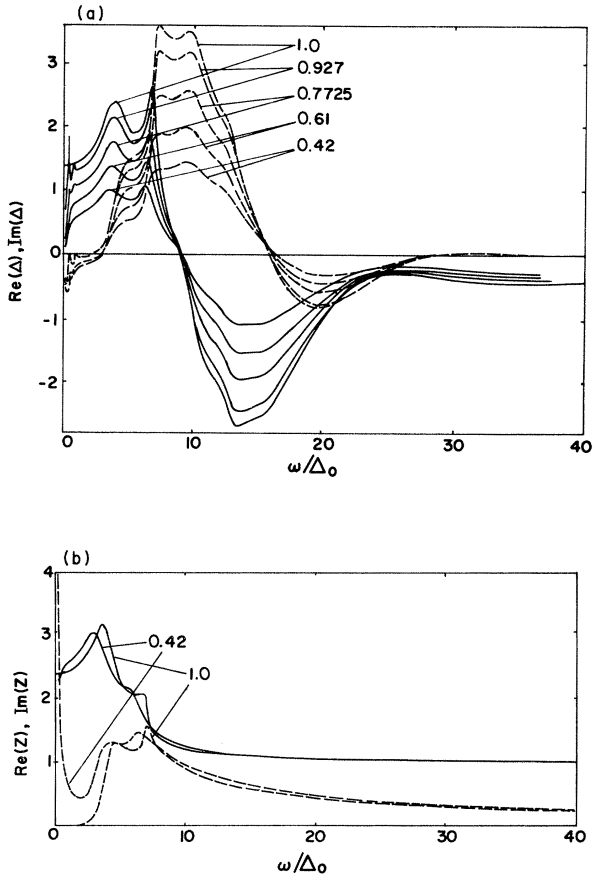

FIG. 2. (a) Real (solid line) and imaginary (dashed line) parts of the complex gap function for pure Pb compared with various Pb-Mn alloys in the model $\epsilon_0=0.25$ and $\epsilon_1=0.8$. Curves are labeled by the ratio of the alloy to the pure-Pb critical temperature $t=T_c/T_{c0}$. (b) Real (solid line) and imaginary (dashed line) part of the renormalization function Z for the same impurity model $\epsilon_0=0.25$ and $\epsilon_1=0.8$ as in (a) for the alloy with critical temperature 0.42 of the pure-Pb temperature T_{c0} compared with the pure-Pb case. Note the small ω dependence of the imaginary part of $Z(\omega)$ in the alloy.

through the simple relation

$$\frac{N(\omega)}{N(0)}=\mathrm{Re}\left[\frac{\omega}{[\omega^2-\Delta^2(\omega)]^{1/2}}\right] \tag{8}$$

even for the case of alloys. Here $N(0)$ is again the electronic density of states for one spin in the normal metal.

In Fig. 3 we show results for the case $\epsilon_0=0.25$ and $\epsilon_1=0.8$ as a function of the energy ω normalized to the pure-Pb gap edge. For $T_c/T_{c0}=0.9985$ we note two very small structures inside the gap region, i.e., $\omega/\Delta_0<1$ centered roughly about 0.25 and 0.75, respectively, with nothing in between. For $T_c/T_{c0}=0.927$ the two structures just described have grown enormously in size both on the horizontal and vertical scales. A region of no states remains at low ω up to approximately 0.05, while a second zero region is observed near 0.5 as well as a nearly zero region before the main sharp rise in $N(\omega)$ starts. This is quite different from the previous results obtained by Schachinger [also included for comparison (dashed curves)] using imaginary-axis solutions with Padé approximants to perform an analytic continuation to the real axis. It is clear that such a technique tends to produce some smearing of the structures below the main gap edge. It even puts a small, but finite, density of states in regions where it should be zero. As the impurity concentration is increased, however, it is seen that the two techniques start giving essentially the same results. This is not unexpected since the curves become progressively smoother and, therefore, much more easily described by Padé approximants which basically employ ratios of polynomials. Our conclusion then is that Padé approximants cannot reproduce in detail the structure below the gap when it consists of separate distinct parts. It is difficult in this technique to describe regions of exactly zero density.

Our next question is to ask how do strong-coupling results compare with weak-coupling results in the region below and around the gap edge for a given set of impurity parameters. Tsang and Ginsberg[11] have employed a multilevel SR-type analysis based on BCS theory to analyze some of their tunneling data of Pb-Mn. For a sample with $T_c/T_{c0}=0.996$ they consider two sets of parameters, namely, for case I,

$$\epsilon_0=0.985,\quad \epsilon_1=0.967,\quad \epsilon_2=0.970\ ,$$

and for case II

$$\epsilon_0=0.959,\quad \epsilon_1=-0.680,\quad \epsilon_2=0.990\ ,$$

and show the quasiparticle density of states below and

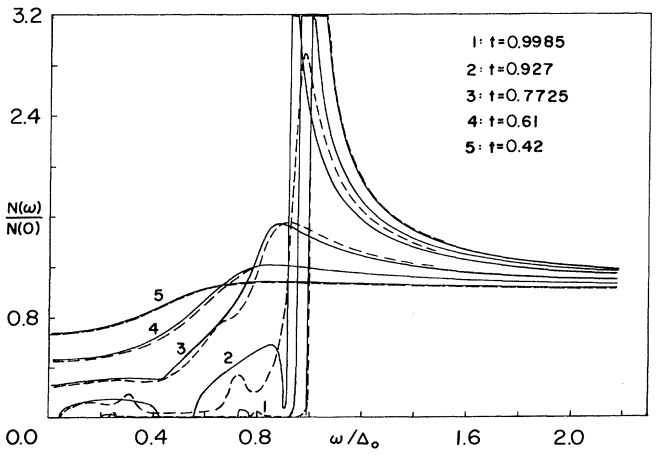

FIG. 3. Comparison of the quasiparticle density of states for a model $\epsilon_0=0.25$ and $\epsilon_1=0.8$ of Pb-Mn alloys obtained in this work using the real-axis formulation of the Eliashberg equations (solid lines) with the previous work of Schachinger (dashed lines) using an imaginary-axis formulation with Padé approximants to analytically continue to the real axis. Various alloys are labeled by the reduced temperature $t=T_c/T_{c0}$ with T_{c0} the pure-Pb critical temperature.

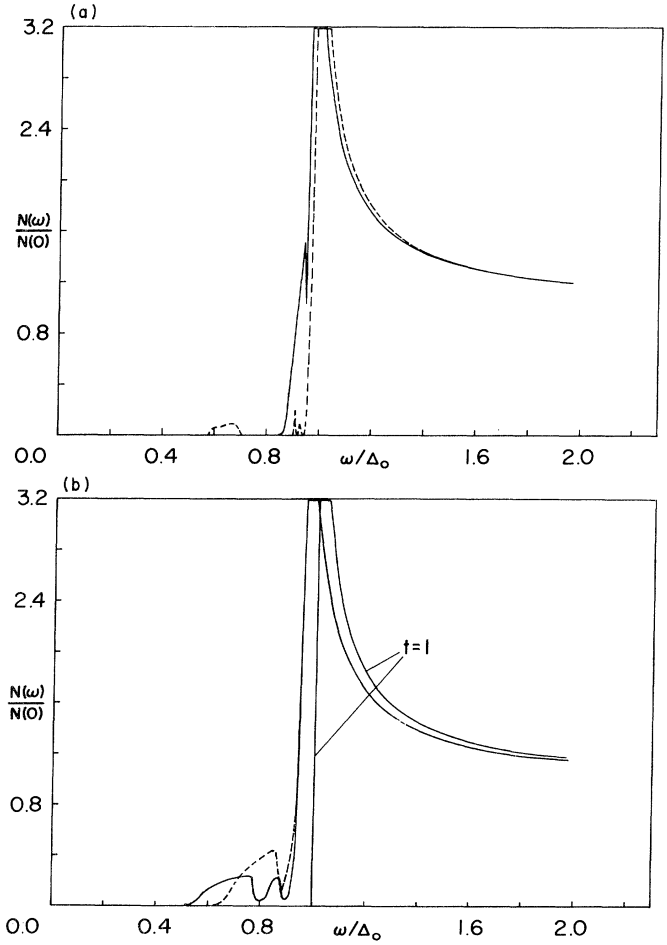

FIG. 4. (a) Quasiparticle density of states for a Pb-Mn alloy with ratio of alloy (T_c) to pure-metal (T_{c0}) critical temperature $t=T_c/T_{c0}=0.996$ obtained from the solution of the Eliashberg equations (1) and (2). Solid line is for the impurity model $\epsilon_0=0.985$, $\epsilon_1=0.967$, and $\epsilon_2=0.970$, while the dashed curve is for $\epsilon_0=0.959$, $\epsilon_1=-0.680$, and $\epsilon_2=0.990$. These two models have been considered by Tsang and Ginsberg in their analysis of tunneling data which they based on a BCS-theory model for the superconducting state. (b) Quasiparticle density of states for an In-Cr alloy with ratio of the alloy (T_c) to pure-metal (T_{c0}) critical temperature $t=T_c/T_{c0}=0.98$ obtained from the solution of the Eliashberg equations (1) and (2). Solid line is for the impurity model $\epsilon_0=0.8944$, $\epsilon_1=0.7289$, and $\epsilon_2=0.9885$, while the dashed curve is for $\epsilon_0=0.9715$, $\epsilon_1=0.9398$, and $\epsilon_2=0.9938$. These two models have been considered by Terris and Ginsberg in their analysis of tunneling data which they based on a BCS theory model for the superconducting state.

near the gap edge for both cases. In Fig. 4(a) we show similar results for $N(\omega)/N(0)$ but now obtained from a solution of the strong-coupling Eqs. (1) and (2). For case I we obtain, as did Tsang and Ginsberg, a structure which merges with the main increase in density of states near the Pb gap edge. Our structure, however, is not as high and considerably broader, extending down to approximately $\omega/\Delta_0=0.87$ as opposed to 0.93 in BCS theory. A similar situation obtains in the second case (dashed line). Right below the main rise near the Pb gape edge, we obtain two small peaks which are smaller in height and less well separated than those of Tsang and Ginsberg, extending, however, to $\omega/\Delta=0.9$ compared with 0.95 for the BCS-theory model. In addition we find a small structure extending from about 0.58 to 0.7 which is very similar in size to that found in BCS theory extending from 0.63 to about 0.74.

To emphasize further the differences between strong-coupling and BCS-theory results we discuss now the impurity concentration estimates coming from Eq. (5) within the two formalisms. For case I we get 27.9 ppm Mn and for case II 96.2 ppm in contrast to the BCS-theory values of 11 and 37 ppm, respectively. Tsang and Ginsberg quote a concentration of 69 ppm for their experiment. We see that the strong-coupling result for case I is still far below the experimental value while for case II it is now above. (The model with only two localized states at $\epsilon_0=0.25$ and $\epsilon_1=0.8$ requires a concentration of 24.8 ppm for a reduced temperature of $t=0.996$.) If we assume case I to be the best description, an actual concentration of 69 ppm Mn would correspond to a reduced critical temperature of $t=0.989$ and thus to $T_{c0}=7.271$ K for the pure-Pb film. This value is not unreasonably high.

We turn now to a comparison of strong coupling with BCS results for the case of indium doped with chromium, alloys analyzed by Terris and Ginsberg.[13] Our strong-coupling results for an alloy with $T_c/T_{c0}=0.98$ with, for case I,

$$\epsilon_0=0.8944,\quad \epsilon_1=0.7289,\quad \epsilon_2=0.9885\ ,$$

and for case II,

$$\epsilon_0=0.9715,\quad \epsilon_1=0.9398,\quad \epsilon_2=0.9938\ ,$$

are found in Fig. 4(b). In case I we obtain two structures in the gap with a low but finite density-of-states region in between, as compared with BCS theory in which case a zero is observed in this region. Further, the lowest structure extends to $\omega/\Delta=0.53$ instead of 0.6. Also the main rise in the density of states starts around 0.9 in our results rather than just below 1 in BCS theory. In case II, a single structure near the main edge is observed but with only about half the height of the BCS-theory result and extends down to 0.65 rather than only 0.88. Also, the main rise is around 0.9 rather than near 1. We conclude from these comparisons that the strong-coupling results are similar to the weak-coupling results below and near the gap edge of the pure metal, but that they differ considerably in detail. If a full Eliashberg theory were used to fit the tunneling data, as did Tsang and Ginsberg and Terris and Ginsberg, somewhat different impurity parameters would result. Also it is clear from Fig. 4 that for a given set of ϵ_l's and fixed T_c/T_{c0} strong coupling predicts a very much larger impurity concentration than BCS theory, indicating that it may be necessary to choose very different impurity parameters should the concentration be known independently. It is perhaps worthwhile emphasizing that in the square-well model $\alpha_c=(1+\lambda)\alpha_c^{\rm BCS}$, which brings the curves in Fig. 1 closer to the exact strong-coupling results.

While it is not our primary aim in this work to compare with tunneling experiments, which would require a variation of the scattering parameters ϵ_l to get the best possible fit to the data, we do present the current-voltage (I-V) characteristics for an aluminum—insulator—Pb-Mn junction at $T=1.08$ K for the alloy with 0.996 considered by Tsang and Ginsberg. The tunneling current is computed from

$$I(V)\propto\int_{-\infty}^{+\infty}\frac{N_{1s}(\omega+eV)}{N_1(0)}\frac{N_{2s}(\omega)}{N_2(0)}[f(\omega)-f(\omega+eV)]d\omega\ ,$$

where $N_{1s}(\omega)/N_1(0)$ and $N_{2s}(\omega)/N_2(0)$ are the quasiparticle densities of states on sides 1 and 2, respectively. In Fig. 5 we show results for cases I and II defined previously and for case III with $\epsilon_0=0.25$ and $\epsilon_1=0.8$. Pure Pb is also shown for comparison. Just as was found by Tsang

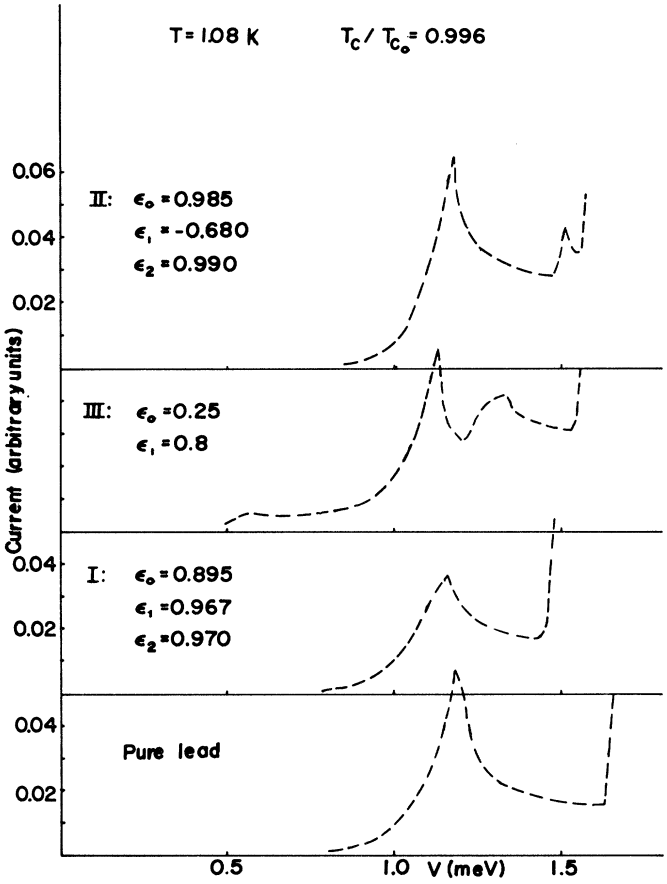

FIG. 5. Current as a function of voltage of an Al—insulator—Pb-Mn junction at $T=1.08$ K for three different models of the scattering parameters ϵ_l. Alloy reduced temperature $T_c/T_{c0}=0.996$. Pure Pb is also shown for comparison.

and Ginsberg, cases I and II do not show enough structure between the cusp at about 1.15 meV and the main rise at the gap edge, while case III shows too much filling in of this energy region. Also, in this last instance, the predicted structure at lower bias is too large. Tsang and Ginsberg state that variation of the ϵ_l's did not lead to a completely satisfactory fit to the data. It would be much too costly to perform an exhaustive search in strong-coupling theory. It is clear from the figure, however, that the theory is well able to handle, with good numerical accuracy, the small structures dealt with in SR theory when the impurity concentration is very low.

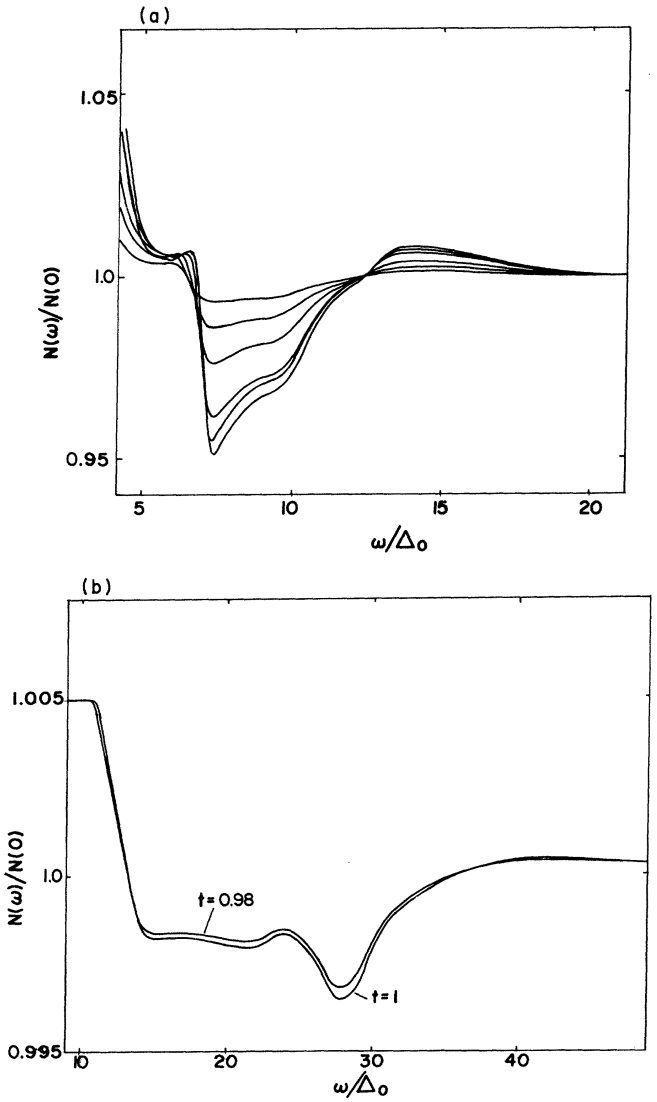

FIG. 6. (a) Quasiparticle density of states for a series of Pb alloys with impurity parameters $\epsilon_1=0.25$ and $\epsilon_2=0.8$ shown in the phonon-energy region. Curves are for the reduced temperatures $t=1$ (pure Pb), 0.9985, 0.927, 0.7725, 0.61, and 0.42. Here t is the ratio of the alloy (T_c) to pure-Pb (T_{c0}) critical temperature and the phonon structure progressively decreases in amplitude as we go through the alloy series. (b) Quasiparticle density of states for pure In and In-Cn alloy with $t=0.98$ where t is the ratio of the alloy (T_c) to the pure-metal (T_{c0}) transition temperature. Alloy parameters are $\epsilon_0=0.8944$, $\epsilon_1=0.7289$, and $\epsilon_2=0.9885$.

IV. INTERPLAY WITH THE PHONON STRUCTURE

So far, we have concentrated in the energy region near and below the pure-Pb or -In gap edge. In the BCS-theory case, this is the only region of significance while in strong-coupling theory another very interesting region is near the phonon energies. As is so well known and exploited to great advantage,[18] structure is observed in the I-V characteristics related to the electron-phonon spectral density $\alpha^2(\omega)F(\omega)$. This structure is used to invert tunneling data and so obtain the spectral density and Coulomb pseudopotential.

In this section we present our results for the quasiparticle density of states in the phonon region. These are shown in Figs. 6(a) and 6(b) for Pb and In, respectively. Concentrating on Pb, for which case more results are shown, we see that as the impurity content is increased, the phonon structure is progressively decreased as well as somewhat shifted. This can be traced back to the gap solutions shown in Fig. 2(a). Formula (8) for the quasiparticle density of states can be written in the form

$$\frac{N(\omega)}{N(0)} \cong 1+\frac{1}{2}\frac{\Delta_1^2(\omega)-\Delta_2^2(\omega)}{\omega^2} \tag{9}$$

when ω is much larger than the gap. In Eq. (9), Δ_1 and Δ_2 are, respectively, the real and imaginary part of the gap. As is seen in the figure both these quantities are progressively reduced as the impurity concentration is increased. This leads to the observed weakening of the phonon effects as the impurity concentration is increased.

V. CONCLUSIONS

We have solved the Eliashberg equations, written on the real axis, for superconducting alloys containing paramagnetic impurities treated in the T-matrix approximation of SR, including several different partial waves in the scattering channel. Comparison of our solutions with previous imaginary-axis Eliashberg solutions supplemented with a Padé-approximant technique to perform the analytic continuation to the real axis, reveals excellent agreement between the two methods when the impurity concentration is sufficiently large that no discontinuous isolated structures occur in the pure-metal gap region. At low concentration the Padé approximants cannot easily reproduce the isolated regions of zero density and tend to smear somewhat the structures within the gap. Comparison with BCS solutions using the same impurity parameters shows qualitative agreement with the general trends but reveals differences in details as to height, position and width of the structure below the gap. Also, the position of the main rise is different in the two approaches.

Our strong-coupling solutions allow us to examine the energy region where phonon effects are observed. This is entirely missing in BCS theory solutions. It is found that large modifications occur with a general weakening of phonon effects as the impurity concentration is increased.

ACKNOWLEDGMENTS

All numerical calculations were performed on the UNIVAC 1100/81 computer of EDV-Zentrum der Technischen Universität, Graz, Austria. We also wish to thank Professor Ginsberg for supplying us with some extended plots of his data. This research was supported by National Science and Engineering Research Council of Canada and by Fonds zur Förderung der wissenschaftlichen Forschung, Project No. 4440.

[1]H. Shiba, Prog. Theor. Phys. 40, 435 (1968).
[2]H. Shiba, Prog. Theor. Phys. 50, 50 (1973).
[3]A. I. Rusinov, Zh. Eksp. Teor. Fiz. Pis'ma Red. 9, 146 (1969) [JETP Lett. 9, 85 (1969)].
[4]A. I. Rusinov, Zh. Eksp. Teor. Fiz. 56, 2043 (1969) [JETP 29, 1101 (1969)].
[5]A. A. Abrikosov and L. P. Gor'kov, Zh. Eksp. Teor. Fiz. 39, 1781 (1960) [Sov. Phys.—JETP 12, 1243 (1961)].
[6]A. N. Chaba and A. D. S. Nagi, Can. J. Phys. 50, 1735 (1972).
[7]S. C. Lo and A. D. S. Nagi, Phys. Rev. B 9, 2090 (1974).
[8]B. Leon and A. D. S. Nagi, J. Phys. F 5, 1533 (1975).
[9]R. C. Shukla and A. D. S. Nagi, J. Phys. F 6, 1765 (1976).
[10]A. B. Kunz and D. M. Ginsberg, Phys. Rev. B 22, 3165 (1980).
[11]J. K. Tsang and D. M. Ginsberg, Phys. Rev. B 21, 132 (1980); B 22, 4280 (1980).
[12]D. M Ginsberg, Phys. Rev. B 20, 960 (1979).
[13]B. D. Terris and D. M. Ginsberg, Phys. Rev. B 25, 3132 (1982).
[14]G. M. Eliashberg, Zh. Eksp. Teor. Fiz. 38, 966 (1960) [Sov. Phys.—JETP 11, 696 (1960)].
[15]E. Schachinger, Z. Phys. B 47, 217 (1982).
[16]E. Schachinger, J. M. Daams, and J. P. Carbotte, Phys. Rev. B 22, 3194 (1980).
[17]H. D. Vidberg and L. W. Serene, J. Low Temp. Phys. 29, 179 (1977).
[18]W. J. McMillan and J. M. Rowell, in *Superconductivity,* edited by R. D. Parks (Dekker, New York, 1969), p. 561.